NASA TECHNICAL
MEMORANDUM

EXPERIMENTAL PERFORMANCE OF CASCADE THRUST REVERSERS AT FORWARD VELOCITY

by Donald A. Dietrich and Roger W. Luidens

Lewis Research Center
Cleveland, Ohio 44135

EXPERIMENTAL PERFORMANCE OF CASCADE THRUST

REVERSERS AT FORWARD VELOCITY

by Donald A. Dietrich and Roger W. Luidens

Lewis Research Center

SUMMARY

A series of static and wind tunnel tests were performed on four cowl cascade thrust reverser configurations which had various reversed jet emission patterns applicable to an externally blown flap STOL aircraft. The work was performed using a model fan which was 14.0 centimeters in diameter and passed a fan mass flow of 2.49 kilograms per second at an approximate fan pressure ratio of 1.22 and fan corrected rotational speed of 35 800 rpm. The tests demonstrated that the reingestion of fan flow significantly reduced the reverser efficiency and that the thrust reverser efficiency was improved by reducing the reversed jet azimuthal emission angle. The reverser efficiency at STOL landing speeds was as high as 0.95; however, configurations with lateral emission were adversely affected by yawing the nacelle at forward velocity. Measurements of the internal static pressure at the stator exit showed significant increases in the local static pressure for configurations with reduced jet emission angles.

INTRODUCTION

A basic requirement of all aircraft is the ability to stop during the landing and aborted takeoff procedures. A variety of jet thrust reversers are regularly used during normal CTOL aircraft operation to augment the braking system because they can substantially retard tire and brake wear; furthermore, under adverse conditions such as wet or icy runways, thrust reversers greatly reduce the ground roll distance.

The application of thrust reversing to STOL operation differs from the case of CTOL primarily because of the shorter field length and higher thrust-to-weight ratio of STOL aircraft. High reverse thrust may well be necessary in emergency operations, such as a misjudged landing or aborted takeoff. If the reverser performance were sufficiently high, it may be possible to use reversers on only two engines of a four-engine airplane

and be able to provide sufficient stopping forces. The possibility also exists that reverser noise may be reduced by the application of a highly efficient reverser system. If the requirement on the system is to provide a specified stopping force, then a highly efficient system may be operated at a reduced throttle setting which implies a lower exhaust jet velocity and thus lower noise.

The thrust reverser configurations considered in this report are cowl-mounted cascade thrust reversers and are applied to a low-pressure-ratio model fan. The particular configurations of interest produce reversed jet patterns with significantly reduced total azimuthal emission angles which imply relatively large areas of circumferential blockage of the exhaust jet. These reverser configurations are particularly applicable to an externally blown flap STOL aircraft because a highly tailored reversed jet flow is required to prevent impingement on an adjacent engine, the fuselage, or the ground. A discussion of STOL aircraft configurations is presented in references 1 and 2, and references 3 to 7 consider the design and testing of various thrust reverser systems.

Very little information is available on the performance of a combined low-pressure-ratio fan and a highly tailored reverser system. The present work was initiated to investigate the performance of a model fan-reverser system. The objective of this study was to determine both the thrust reverser efficiency and the variation of the fan duct static pressure. The study was made for a range of azimuthal emission angles of approximately 160° to 320° and fan speeds of 90 and 100 percent of design speed. Wind tunnel tests were conducted for a range of yaw angles from 0° to 90° and forward velocities from static to 35 meters per second

SYMBOLS

b	blocker door position
C_D	discharge coefficient, flow area (forward)/total reverser area
d	passage diameter in reverser section
N	corrected fan rotational speed
p	static pressure at stator exit
p_o	free-stream static pressure
V_o	free-stream velocity
$\dot{w}$	corrected fan weight flow
η	thrust reverser efficiency

ψ yaw angle

θ azimuthal angle

APPARATUS

Thrust Reverser Model

Figure 1(a) is a sketch of the model fan and nacelle with the cascade thrust reverser used in the test series.

Fan and inlet. - The fan had a fan tip diameter of 14.0 centimeters, and at the design rotational speed of 35 800 rpm passed a mass flow of 2.49 kilograms per second at a pressure ratio of 1.22.[1] The fan was driven by a tip turbine which at the fan design speed required a mass flow of 0.47 kilogram per second of unheated air at a pressure of 2590 kilonewtons per square meter in the turbine plenum. Downstream from the tip turbine and rotor, the drive and fan flows mix. Here the passage outer diameter is 15.2 centimeters and the centerbody diameter is 7.46 centimeters. Detailed information on the basic fan performance with various inlets and exits is given in references 8 and 9.

The total length of the inlet and fan combination from inlet highlight to stator exit was 11.7 centimeters. The contour of the fan inlet lip was made up of quadrants of two 2:1 ellipses as illustrated in figure 1(b). The inlet contraction ratio, which is the highlight-to-throat area ratio, was 1.29.

Thrust reverser section. - The thrust reverser section, figure 1(a), consisted of eight replaceable cascade sectors, the forward and aft housing rings, and two axial support rails located 180° apart. Each cascade sector subtended an azimuthal angle of 42.5° and was replaceable by a solid sector which provided azimuthal blockage of the flow for some configurations. Since each sector contained end rails, the azimuthal flow angle of each sector was 40.2°. The combined fan and drive flow was turned through the cascade reversers by a blocker door which had a forward sloping surface of 45° and seals to prevent flow leakage axially. The blocker door was axially translatable, thus making the effective fan exit area and mass flow adjustable.

The cascade reverser blades were designed according to the following procedure. To reduce losses through the cascade blades, it was estimated that a minimum Reynolds number of 10^5 based on the blade chord and the fan duct velocity was required. Specifying this value for the case of the fan operating at 60 percent of the design thrust gave a blade chord length of 1.27 centimeters. A solidity of 1.3, an approximate turning angle

---

[1]When the fan was operated at a rotational speed of 32 000 rpm, the fan pressure ratio was 1.18.

of 135°, and a 15 percent thick blade contour having a camber of 110° (based on data in ref. 10) were selected. The blade section is illustrated in figure 1(c). The angle between the chord line of the reverser blade and the fan centerline was 75°. Accounting for the radial divergence in flow area through the blades, this design incorporates a cross-sectional flow passage that converges. This feature helps avoid flow separation. From the blade design and the information in reference 11, the cascade discharge coefficient was estimated to be 0.55. Allowing for a 15 percent variation in the discharge coefficient, the number of blades and length of the cascade section were then determined such that the combined fan and turbine flow would pass through the reverser configuration with the lowest total emission angle.

Instrumentation. - The instrumentation is also illustrated in figure 1(a). A single component load cell was located in the model centerbody and used to measure the total axial force during wind tunnel tests. The model centerbody also contained a light sensitive cell to measure fan rotational speed.

Seven static pressure taps were located in the outer passage wall between the stator exit plane and the thrust reverser section. These were located azimuthally midway between stator trailing edges.

Test Facilities

Two test facilities were used during the test series: the static test stand (ref. 8) and the Lewis 2.74- by 4.57-meter low speed wind tunnel (ref. 12).

Static test stand. - The static stand, shown in figure 2, was constructed to support the fan with its thrust reverser, a bellmouth inlet, and a barrier between the reverser section and inlet. The bellmouth was located 7.5 fan diameters forward of the fan stator exit plane and connected to the fan by a cylindrical passage. Measurements of the static pressure on the surface of the cylindrical passage were used to determine the fan mass flow assuming a total pressure recovery of one. A 0.6- by 1.2-meter barrier was used to prevent reingestion of the reversed flow and was located 4.3 fan diameters forward of the stator exit plane.

Low speed wind tunnel. - The features of the Lewis 2.74- by 4.57-meter low speed wind tunnel are detailed in reference 12. The installation of the model fan and thrust reverser in the wind tunnel is shown in figure 3. The high pressure air supply line utilized two large radius turns to minimize the extraneous force it could apply to the model.

4

PROCEDURE

Thrust Reverser Efficiency

The thrust reverser efficiency was calculated according to the following procedure. Static tests were performed to adjust the blocker door position to match the fan weight flows of a standard forward thrust exit and the reverser configurations. This blocker door position was used to perform static and wind tunnel tests to determine the thrust reverser efficiency which was the ratio of the reversed thrust measured along the fan axis at any forward velocity and yaw angle to the forward thrust at static conditions for the same fan corrected rotational speed. Measurement of the fan weight flow was not made during the wind tunnel tests.

Test Configurations

Table I contains a schematic representation of the five configurations tested: one configuration using a standard exit and four reverser configurations. The standard exit consisted of a constant area annular flow passage followed by an aerodynamically tapered centerbody. This exit produced the forward thrust that was the basis for calculating the thrust reverser efficiency.

For the thrust reverser configurations, the model allowed both the number of cascade sectors and the blocker door position to be varied. Thus, the model could be arranged to produce reversed jet flows of varying emission patterns and aspect ratios while maintaining the same fan weight flow and turning angle with respect to the fan axis. The first reverser configuration used all eight cascade sections and had a total azimuthal emission angle of 321.6^{o} as noted in the fourth column of table I. The second thrust reverser had approximately 33 percent of the circumference blocked giving a total emission angle of 241.2^{o}. The remaining two configurations had more than half the circumference blocked giving a total emission angle of 160.8^{o}. The difference between the last two was the geometrical arrangement of the emission pattern, as shown in table I.

Blocker Door Position

The static test stand was used to measure the fan rotational speed and fan weight flow for various blocker door positions on each configuration. These tests were performed so that the blocker door position which reasonably matched the weight flow of

the standard exit could be determined. Figure 4 presents the variation of corrected fan weight flow with blocker door position for all the thrust reverser configurations and at two fan rotational speeds. The weight flow was normalized by the corrected fan weight flow using the standard exit. The blocker door position b was measured as shown in figure 1(a) and normalized by the thrust reverser internal diameter d. A second abscissa shows the ratio of the circumferential emission area to the standard exit annular flow area. For three thrust reverser configurations, it was possible to match the standard exit weight flow (ordinate equal to unity) within 2 percent. However, for the configuration with the unsymmetrical and highly reduced angle of emission, the maximum weight flow that could be achieved with the present model was 85 percent of the standard exit weight flow.[2] Based on these measurements, the blocker door positions which were selected for the subsequent thrust reverser tests are indicated by tick marks on figure 4 and listed in the fifth column of table I.

As noted previously, the high pressure turbine drive air was unheated and, therefore, exhausted from the turbine at well below 200 K. As a result, ice collected in the exit region of the fan. Because of the ice formation and the possibility that the blocker door may not be located at the leading edge of a cascade blade, it was estimated that the weight flow could not be set and maintained closer than 2 percent.

Wind Tunnel Tests

The tests which were performed in the low speed wind tunnel used the configuration shown in figure 3. The ground side of the load cell in the fan nacelle model was mounted to a vertical post which could be remotely rotated to achieve a yaw angle. A single blocker door position for each configuration was used based on the static test stand results. The tests were conducted by setting the wind tunnel speed, setting the fan rotational speed, and then varying the model yaw angle in increments from 0° to 90°.

RESULTS AND DISCUSSION

Static Reverser Efficiency

The last two columns of table I present the static thrust reverser efficiency with and without the barrier installed. The data taken with the barrier installed using the

---

[2]Furthermore, in comparing reverser efficiencies in subsequent sections, it should be remembered that the 15 percent lower mass flow of this configuration represented approximately the same percentage reduction of reverse thrust.

same model fan, static test stand, and bellmouth inlet as this report were reported in reference 8. The data without the barrier were taken using the wind tunnel configuration shown in figure 3. The two sets of data show a significant reduction of the thrust reverser efficiency in every case when the barrier was not installed. In spite of differences in inlet geometry, the reduction of reverser efficiency was caused primarily by the reingestion of the reversed exhaust flow. There are a number of reports that consider the effect of hot gas reingestion which reduces engine thrust and may cause engine surge (e.g., ref. 4). Since there was no temperature rise in the exhaust flow for the present tests, the effect observed is purely one of airflow recirculation. While there was a small temperature rise of compression associated with the model fan pressure ratio, this was neutralized by the cold turbine exhaust air. The data of table I also indicate that the effect due to reingestion was reduced as the total thrust reverser azimuthal emission angle was reduced.

Effect of Forward Velocity on Efficiency

Figure 5 presents the variation of thrust reverser efficiency as a function of free-stream velocity for two yaw angles and two fan rotational speeds. There is a general trend for efficiency to increase with a decrease in the azimuthal emission angle; and, as was the case at static conditions, the relative values of the efficiencies of the four configurations are determined primarily by the degree to which recirculation occurred, where the degree of recirculation was affected by the total emission angle, forward velocity, and yaw angle. The increase in thrust reverser efficiency with forward velocity for a given configuration was due to the increase in inlet ram drag and base drag with forward speed and to any reduction of the amount of exhaust flow being reingested. For the reduced emission configurations, the reverser efficiency at a forward velocity increased slightly as the fan rotational speed was reduced due to the relative increase of the ram and base drags.

The highest thrust reverser efficiency observed in the present test series was 0.95 and occurred at the condition ($\psi = 0^{\circ}$, $N = 32\ 000$ rpm, and $V_{o} = 33$ m/sec) for a configuration with a total emission angle of 160.8° divided into two sectors oriented 180° apart.

Effect of Yaw Angle on Efficiency

Figure 6 shows the effect of yaw angle on thrust reverser efficiency at a constant free-stream velocity for two fan rotational speeds. For the configurations with high

efficiency which implies little or no recirculation, the efficiency decreased with increasing yaw angle. This is attributable to the decrease in the component of the inlet momentum along the fan axis and any decrease of inlet performance with increasing yaw angle. For the configurations with the lower efficiency and large recirculation, flow angle has little effect on the efficiency.

An additional indication of the effect of recirculation of the exhaust flow is shown in figure 7. Wind tunnel tests were performed with two orientations of the last reverser configuration. The model thus far described was oriented so that the exhaust flow was emitted above and below the plane in which the yaw angle occurred. In the second orientation, the model was rotated 90° about the fan axis so that the exhaust flow was emitted in the plane of the yaw angle. The data were normalized to the reverser efficiency at $\psi = 0^{\circ}$ because of small differences in the zero yaw angle conditions. As the yaw angle was increased, the reverser efficiency of the original orientation, with exhaust in a plane normal to the yaw angle plane, was essentially constant while the reverser efficiency of the rotated orientation was reduced by more than 15 percent at a yaw angle of 45°.

Fan Exit Static Pressures

Figure 8 presents the azimuthal variation of the internal static pressure between the stator exit plane and the reverser section. In all cases, the static pressure is normalized by the free-stream static pressure. For a uniform fully circumferential exhaust discharge, no circumferential variation in the static pressure was expected. The small variations in static pressure for the configuration which has a 321.6° emission angle show the effect of the axial support rails at $\theta = 0^{\circ}$ and 180°. For the configuration with approximately 95° blockage at the bottom of the model, there was a large rise in static pressure in the vicinity of the blockage. For the next configuration with 180° of blockage, both the extent and magnitude of the static pressure rise increased. Breaking the same circumferential blockage into two sectors significantly reduced the static pressure variation. The data of figure 8 also show that the internal static pressure variation is essentially uneffected by the free-stream flow velocity (fig. 8(a)), the flow angle (fig. 8(b)), or fan rotational speed (fig. 8(c)). In general, the internal static pressure distribution was determined only by the thrust reverser geometry.

SUMMARY OF RESULTS

The experimental investigation of the performance of a fan-cascade thrust reverser system was conducted on a model which generated various reversed jet emission pat-

terns. The main results of this investigation may be summarized as follows:

1. Thrust reverser efficiencies as high as 0.95 were attained at typical STOL landing velocities. The maximum value occurred at free-stream velocity $V_0 = 33$ meters per second for a configuration with a total emission angle of 160.8^o divided into two sectors oriented 180° apart.

2. The thrust reverser efficiency was significantly reduced whenever recirculation of fan exhaust flow occurred. A 43 percent loss of reversed thrust occurred when the exhaust flow of the full emission reverser recirculated.

3. The thrust reverser efficiency was improved and recirculation reduced by reducing the jet total azimuthal emission angle.

4. The reverser efficiency of configurations with emission from the sides of the nacelle was adversely affected by yawing the nacelle at forward velocity.

5. For configurations with partial circumferential emission, there was a significant increase in the internal static pressure in the vicinity of the blocked areas. A maximum value of the stator exit static pressure ratio of 1.18 occurred at a fan rotational speed of 36 000 rpm for a configuration with a total emission angle of 160.8^o.
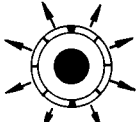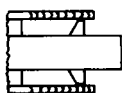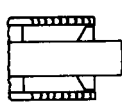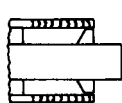
Lewis Research Center,
    National Aeronautics and Space Administration,
        Cleveland, Ohio, October 4, 1972,
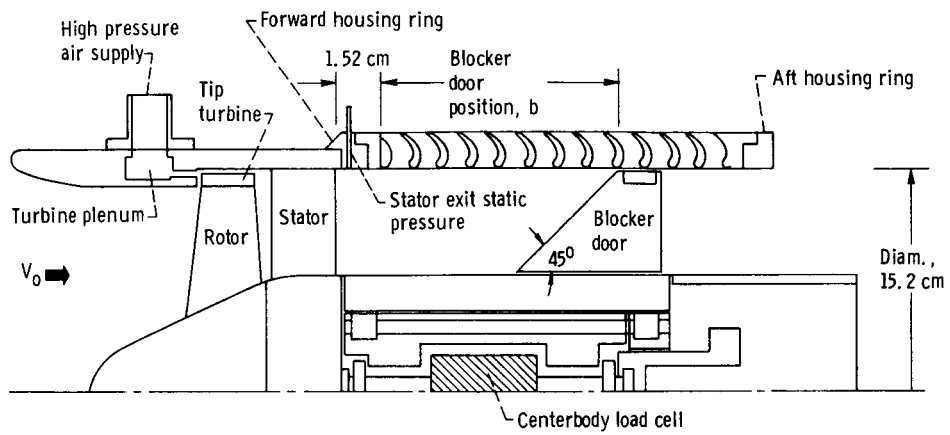   501-24.

REFERENCES

1. Sanders, Newell D.; Diedrich, James H.; Hassel, James L., Jr.; Hickey, David H.; Luidens, Roger W.; and Stewart, Warner L.: V/STOL Propulsion. Aircraft Propulsion. NASA SP-259, 1971, pp. 135-168.

2. Vogler, Raymond D.: Wind-Tunnel Investigation of a Four-Engine Externally Blowing Jet-Flap STOL Airplane Model. NASA TN D-7034, 1970.

3. Poland, Dyckman T.: The Aerodynamics of Thrust Reversers for High Bypass Turbofans. Paper 67-418, AIAA, July 1967.

4. Tolhurst, William H., Jr.; Hickey, David H.; and Aoyagi, Kiyoshi: Large-Scale Wind-Tunnel Tests of Exhaust Ingestion Due to Thrust Reversal on a Four-Engine Jet Transport During Ground Roll. NASA TN D-686, 1961.

5. Wood, Stuart K.; and McCoy, Joe: Design and Control of the 747 Exhaust Reverser Systems. Paper 690409, SAE, Apr. 1969.

6. Lennard, Dean J.: Design Features of the CF6 Engine Thrust Reverser and Spoiler. Paper 690411, SAE, Apr. 1969.

7. Gutierrez, Orlando A.; and Stone, James R.: Preliminary Experiments on the Noise Generated by Target-Type Thrust Reverser Models. NASA TM X-2553, 1972.

8. Lopiccolo, Robert C.: Tests of Cascade Thrust Reversers on a 5.5-Inch Diameter Axial Fan. Rep. 789, Tech Development, Inc., Sept. 1971.

9. Anon.: Performance of a 5.5-Inch Diameter Axial Fan with Various Inlets and Exits. Rep. 708-1, Tech Development, Inc., Mar. 1970.

10. Dunavant, James C.; and Erwin, John R.: Investigation of a Related Series of Turbine-Blade Profiles in Cascade. NACA TN 3802, 1956.

11. Thompson, J. D.: Thrust Reverser Effectiveness on High Bypass Ratio Fan Power-plant Installations. Paper 660736, SAE, Oct. 1966.

12. Yuska, Joseph A.; Diedrich, James H.; and Clough, Nestor: Lewis 9-by-15-foot V/STOL Wind Tunnel. NASA TM X-2305, 1971.
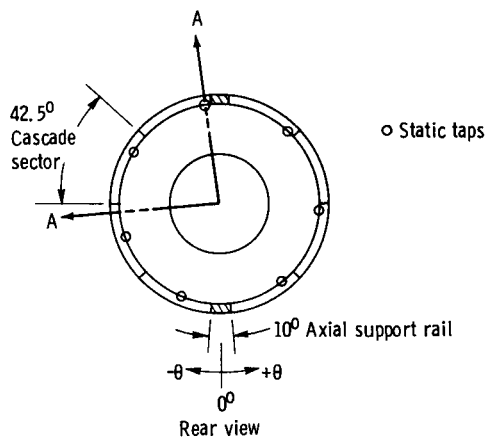
TABLE I. - CONFIGURATIONS TESTED AND STATIC THRUST REVERSER EFFICIENCIES

Exit configuration identification	Configuration schematic		Total emission angle, deg	Normalized blocker door position, b/d	Static thrust reverser efficiency (N = 36 000 rpm)	
	Side view	Rear view			With barrier[a]	Without barrier
Standard exit			-----	----	----	----
Full emission reverser			321.6	0.37	0.74	0.42
Partial emission reverser			241.2	0.59	0.69	0.58
Partial emission reverser			160.8	0.75	----	0.54
Partial emission reverser			160.8	0.75	0.65	0.60
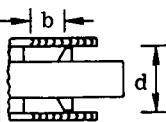
[a]Based on data reported in ref. 8.

Section A-A

(a) Fan, inlet, and thrust reverser section.

Figure 1. - Apparatus.

Coordinates			
X/L	Y/L	X/L	Y/L
0.0	0.0	-0.985	0.305
-.250	.0	-1.0	.375
-.305	.005	-.985	.425
-.410	.015	-.950	.460
-.505	.030	-.880	.485
-.600	.055	-.820	.495
-.700	.090	-.750	.50
-.795	.135	-.250	.50
-.880	.185	0.0	.50
-.950	.255		
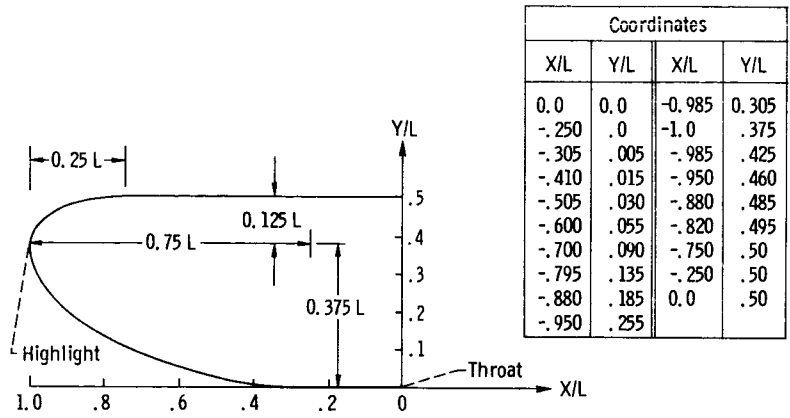
(b) Inlet lip design.
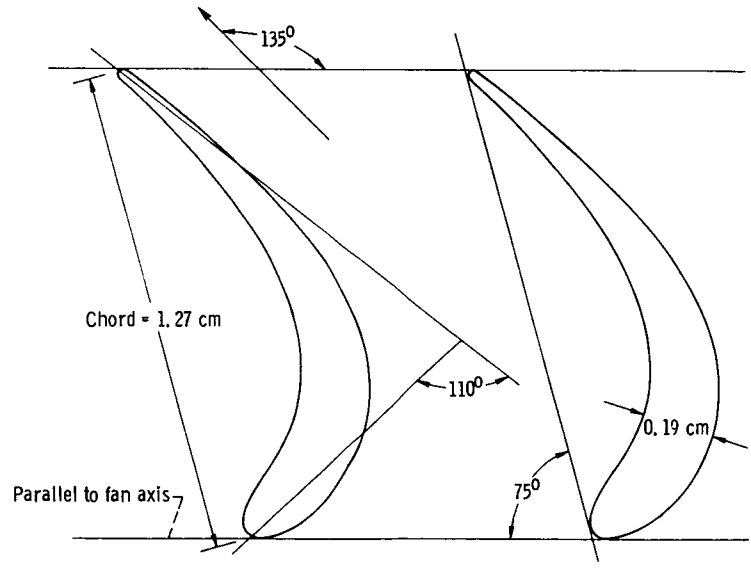
(c) Thrust reverser blade section.

Figure 1. – Concluded.

13
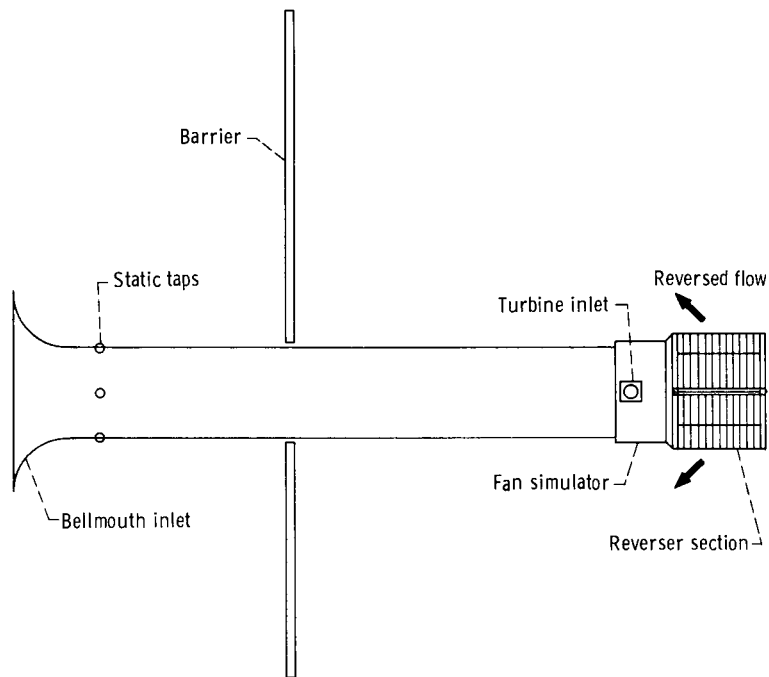
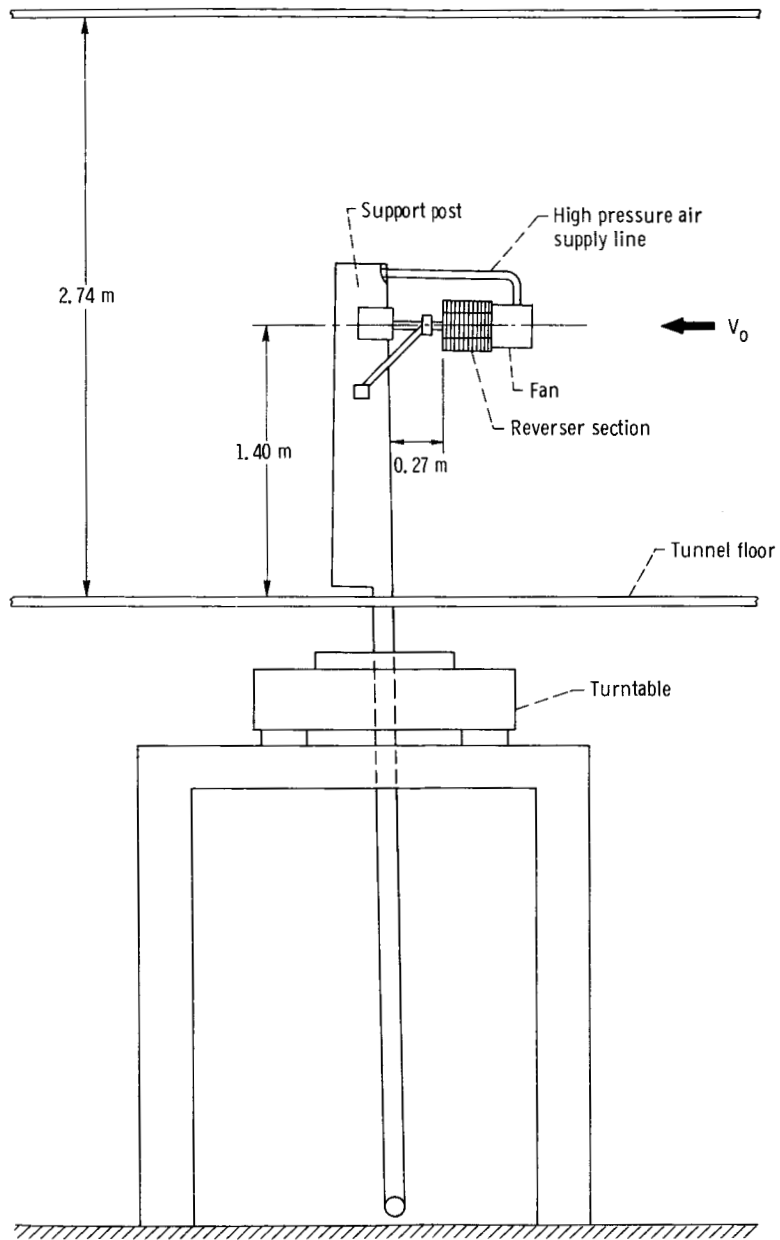Figure 2. - Schematic of static test stand.

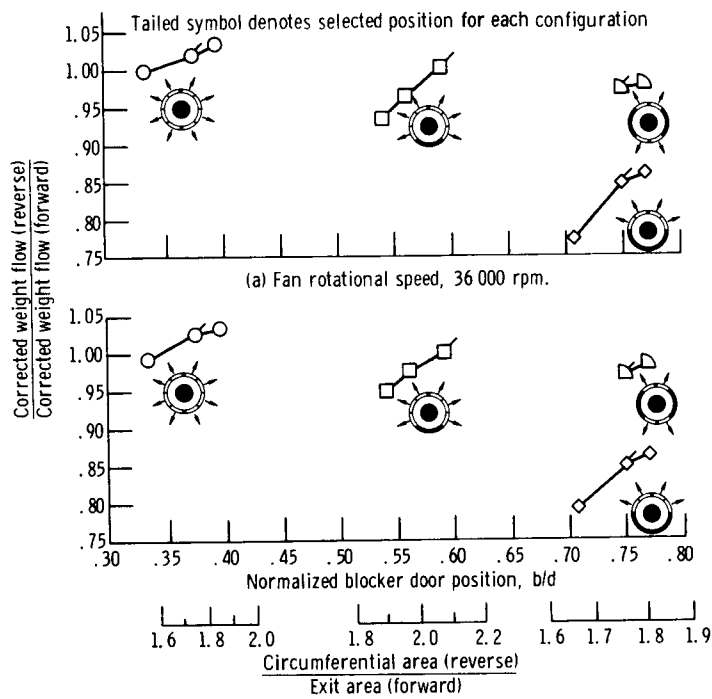Figure 3. - Thrust reverser configuration located in low speed wind tunnel.

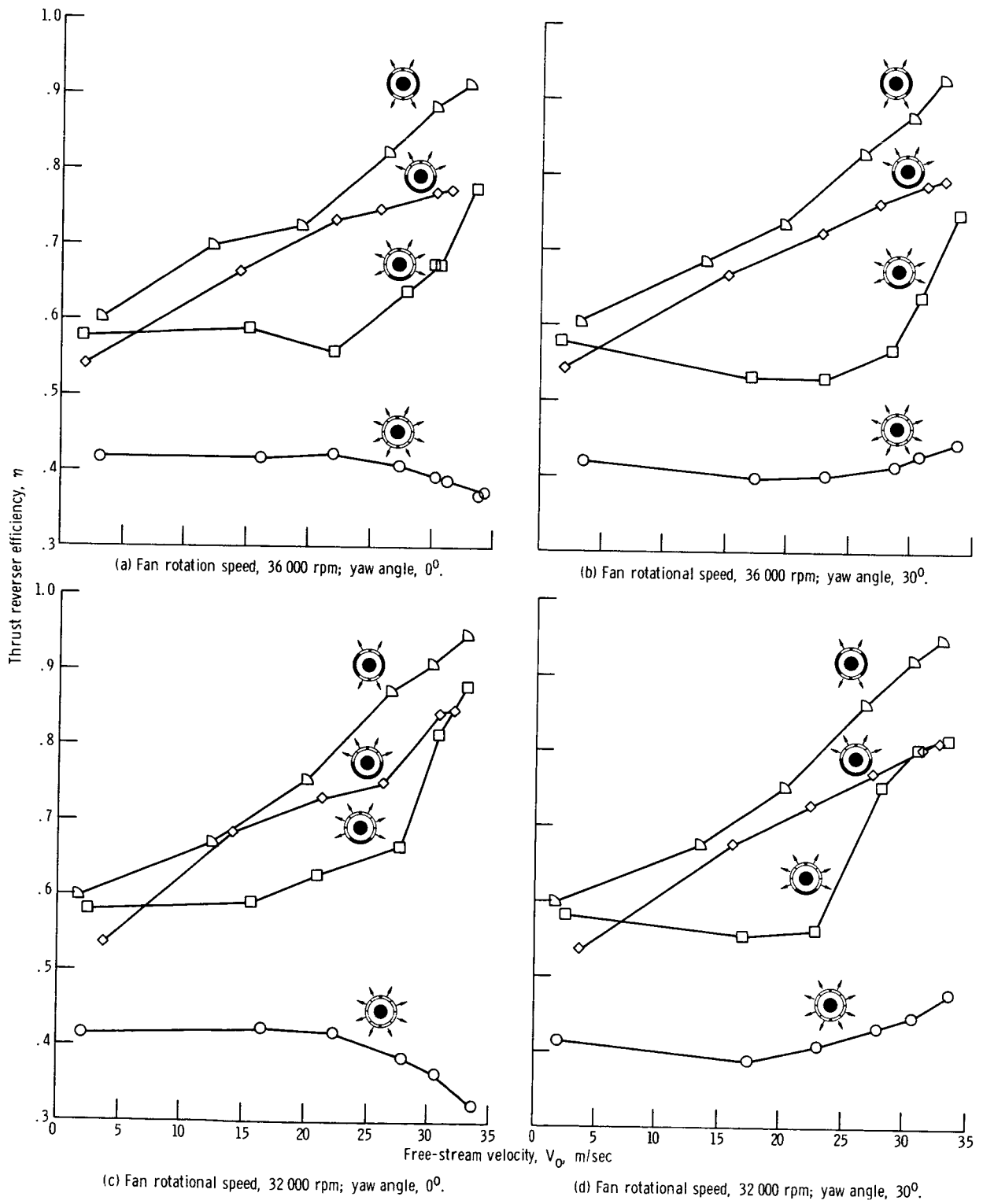Figure 4. - Variation of corrected fan weight flow with blocker door position.

(a) Fan rotation speed, 36 000 rpm; yaw angle, 0°.

(b) Fan rotational speed, 36 000 rpm; yaw angle, 30°.

(c) Fan rotational speed, 32 000 rpm; yaw angle, 0°.

(d) Fan rotational speed, 32 000 rpm; yaw angle, 30°.

Figure 5. - Variation of thrust reverser efficiency with forward velocity for several configurations.

17

(a) Fan rotational speed, 36 000 rpm.
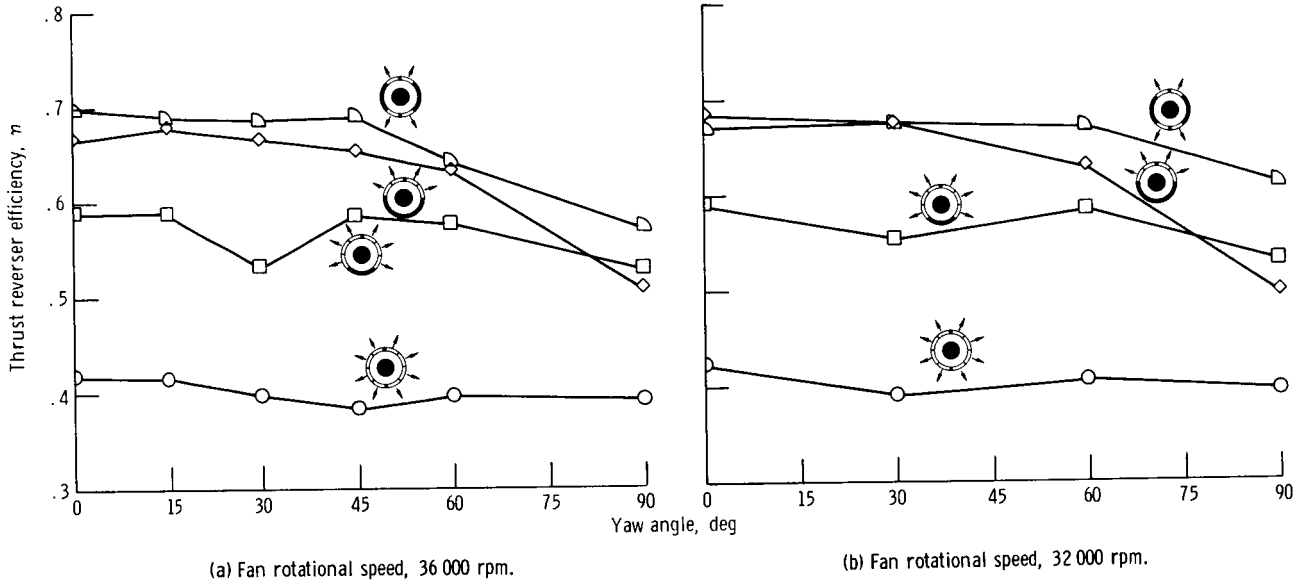
(b) Fan rotational speed, 32 000 rpm.

Figure 6. - Variation of thrust reverser efficiency with yaw angle for several configurations. Free-stream velocity, 16 meters per second.
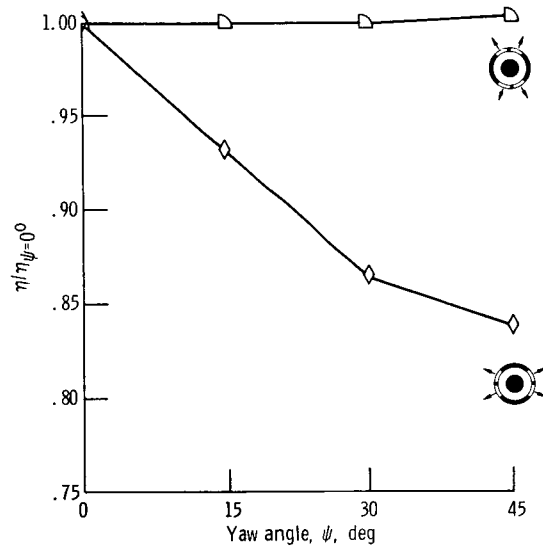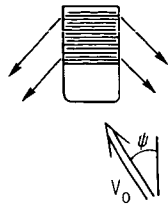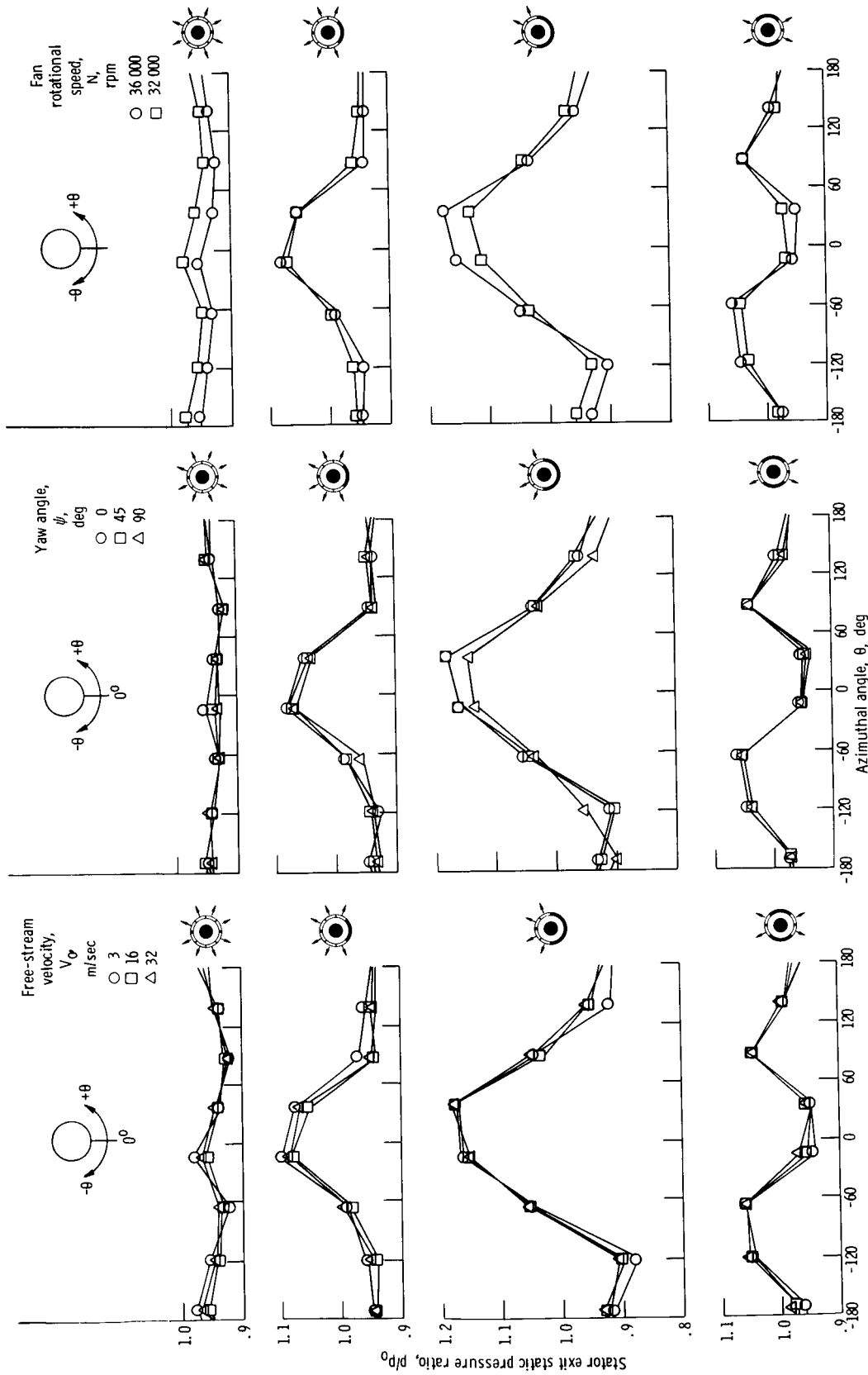
Figure 7. - Variation of relative thrust reverser efficiency with yaw angle for two configurations. Fan rotational speed, 36 000 rpm; free-stream velocity, 16 meters per second.

Figure 8. – Variation of stator exit static pressure with azimuthal angle for several configurations and test conditions.

(a) Effect of forward velocity. Fan rotational speed, 36 000 rpm; yaw angle, 0°.

(b) Effect of yaw angle. Fan rotational speed, 36 000 rpm; free-stream velocity, 16 meters per second.

(c) Effect of fan rotational speed. Yaw angle, 0°; free-stream velocity, 16 meters per second.

20

1. Report No. NASA TM X-2665	2. Government Accession No.	3. Recipient's Catalog No.
4. Title and Subtitle EXPERIMENTAL PERFORMANCE OF CASCADE THRUST REVERSERS AT FORWARD VELOCITY		5. Report Date February 1973
		6. Performing Organization Code
7. Author(s) Donald A. Dietrich and Roger W. Luidens		8. Performing Organization Report No. E-7125
9. Performing Organization Name and Address Lewis Research Center National Aeronautics and Space Administration Cleveland, Ohio 44135		10. Work Unit No. 501-24
		11. Contract or Grant No.
12. Sponsoring Agency Name and Address National Aeronautics and Space Administration Washington, D.C. 20546		13. Type of Report and Period Covered Technical Memorandum
		14. Sponsoring Agency Code

15. Supplementary Notes

16. Abstract

A series of static and wind tunnel tests were performed on four cowl cascade thrust reverser configurations which had various reversed jet emission patterns applicable to an externally blown flap STOL aircraft. The work was performed using a model fan which was 14.0 cm in diameter and passed a fan mass flow of 2.49 kg/sec at an approximate fan pressure ratio of 1.22 and fan corrected rotational speed of 35 800 rpm. The tests demonstrated that the reingestion of fan flow significantly reduced the reverser efficiency and that the thrust reverser efficiency was improved by reducing the reversed jet azimuthal emission angle. The reverser efficiency at STOL landing speeds was as high as 0.95; however, configurations with lateral emission were adversely affected by yawing the nacelle at forward velocity. Measurements of the internal static pressure at the stator exit showed significant increases in the local static pressure for configurations with reduced jet emission angles.

17. Key Words (Suggested by Author(s)) Thrust reversers Cascades Thrust reversing Wind tunnel tests Propulsion systems	18. Distribution Statement Unclassified - unlimited		
19. Security Classif. (of this report) Unclassified	20. Security Classif. (of this page) Unclassified	21. No. of Pages 21	22. Price* $3.00